



2950 Niles Road, St. Joseph, MI 49085-9659, USA
269.429.0300 fax 269.429.3852 hq@asabe.org www.asabe.org

An ASABE Meeting Presentation

DOI: 10.13031/aim.20152177429

Paper Number: 152177429

Commissioning of a Novel Animal Thermal Environment Replication and Measurement System

Brett C. Ramirez¹, Graduate Research Assistant, **Steven J. Hoff¹**, Professor, **Yun Gao^{1,2}**, Visiting Scholar, and **Jay D. Harmon¹**, Professor

¹Department of Agricultural and Biosystems Engineering, Iowa State University, Ames, IA, USA

²College of Engineering Huazhong Agricultural University and the Cooperative Innovation Center for Sustainable Pig Production, Wuhan, China

Written for presentation at the
2015 ASABE Annual International Meeting
Sponsored by ASABE
New Orleans, Louisiana
July 26 – 29, 2015

Abstract. Thermal environment (TE) in livestock production systems effects the animal's thermal comfort, feed efficiency, and the producer's operating costs. Accurate assessment of the radiative component of TE requires Mean Radiant Temperature (t_{mr}) measurement with a Black Globe Thermometer (BGT); however, these devices are cost prohibitive (if multiple are needed), have limited commercial availability, and lack confidence for a range of conditions commonly found in a swine facility. The objectives were to design, construct and commission a novel and well-documented TE simulation system named Animal Thermal Environment Replication and Measurement System (AThERMS). Simulations of different combinations of dry-bulb temperature, relative humidity, and airspeeds while independently controlling chamber surface temperature (t_s) can be evaluated. AThERMS is a 1.04 x 1.17 x 1.04 m chamber inside a large Insulated Enclosure (IE) where air supplied by an air handling unit provides unique TEs to both AThERMS and the IE. Commissioning of AThERMS prior to BGT assessment included a qualitative (smoke visualization) and quantitative (three-dimensional traverse and CFD model) velocity characterization in the central region of the chamber and verification of similar and stable t_s for all six surfaces. Analysis of velocity contours sliced in different x, y, z planes surrounding the BGT at three nominal flowrates indicated steady patterns and helped guide placement of the airspeed sensor used to derive the impact of convection on measured BGT temperature. Results also showed at three nominal t_s (13°C, 23°C, and 33°C), during a 2 h steady state operation, that maximum mean difference between any two t_s measured by six digital IR sensors was 0.26°C with standard deviations less than 0.11°C. Determination of the time constant (τ) for cooling and heating the surfaces showed the time to reach steady-state (3τ , ~95%) to be 85.4 and 42 min, respectively. AThERMS can be used to simulate different TEs a housed animal may experience and function as a reference to calibrate or verify TE measurements.

Keywords. black globe, environment, livestock, thermal, radiation.

The authors are solely responsible for the content of this meeting presentation. The presentation does not necessarily reflect the official position of the American Society of Agricultural and Biological Engineers (ASABE), and its printing and distribution does not constitute an endorsement of views which may be expressed. Meeting presentations are not subject to the formal peer review process by ASABE editorial committees; therefore, they are not to be presented as refereed publications. Citation of this work should state that it is from an ASABE meeting paper. EXAMPLE: Author's Last Name, Initials. 2015. Title of Presentation. ASABE Paper No. ---. St. Joseph, Mich.: ASABE. For information about securing permission to reprint or reproduce a meeting presentation, please contact ASABE at rutter@asabe.org or 269-932-7004 (2950 Niles Road, St. Joseph, MI 49085-9659 USA).

Introduction

Supply and control of the optimum Thermal Environment (TE) inside livestock buildings is needed to address future food security demands without neglect of environmental impact. Thermal environment influences animal well-being, growth performance, feed conversion efficiency, and places the animal at risk for adverse health effects (Boon & Wray, 1989; DeShazer & Yen, 2009; Gentry, McGlone, Miller, & Blanton, 2004; Hillman, 2009; Mount, 1975; Randall, 1993; Straw, Zimmerman, D'Allaire, & Taylor, 1999). In addition, about 25% of the total energy used in conventional swine production systems (farrow to finish) is attributed to building operation (Lammers et al., 2012). Spatial and temporal distribution of TE varies considerably inside buildings (Bjerg, Svidt, Zhang, & Morsing, 2000; Jerez, Wang, & Zhang, 2014; Wang, Zhang, Sun, & Wang, 2008; Zhang, Barber, & Ogilvie, 1988) and requires accurate quantification, such that the most effective management strategies and building design can be implemented.

Thermal environment describes the parameters that influence heat exchange (i.e., convective, conductive, radiative, and evaporative) between an animal and its surroundings (ASHRAE, 2013; Curtis, 1983; DeShazer, 2009). Measureable parameters of TE include dry-bulb temperature (t_{db}), relative humidity (RH), airspeed, and mean radiant temperature (t_{mr}). Dry-bulb temperature is often the main parameter used to describe and control TE; however, it exclusively impacts convective heat loss. While RH indirectly effects latent heat loss, it does quantify the relation between water vapor pressure (directly drives latent heat exchange) and saturation vapor pressure. Airspeed influences convective heat transfer and can substantially increase heat loss (beneficial in a hot t_{db} ; negative in a cold t_{db}). Lastly, t_{mr} is the uniform temperature of the surroundings in which radiant heat transfer from the animal's surface equals that in the actual surroundings. Due to the difficulty to instrument, potentially complex computation, and relative unknown conclusions from the data determining t_{mr} is often neglected livestock facilities; despite, Bond et al. (1952), Mount (1967), Mount (1964), and Beckett (1965) having showed radiative heat losses to be a substantial source of heat loss from swine.

The net exchange of diffuse thermal radiation between two objects is determined by the radiation flux of each object and the shape (view or angle) factor between the objects. Shape factors describe the fraction of thermal radiation departing one object incident on another object (ASHRAE, 2013). Calculation of shape factors can be computationally intensive for complex environments (Alfano, Dell'isola, Palella, Riccio, & Russi, 2013), but for basic geometries, many derivations exist; thus, direct measurement of t_{mr} is preferred. Often, t_{mr} is measured by the Black-Globe Thermometer (BGT; Bedford & Warner, 1934). Developed by Vernon (1932), the BGT is simply a hollow sphere painted flat (matte) black with a t_{db} sensor at the center. The standard BGT is a 0.15 m (6 in.) diameter copper sphere with thin walls with a response time between 20 and 30 min (Hellon & Crockford, 1959). Albeit, a BGT can be any diameter, the standard may be impractical for some applications; however, as diameter decreases, airspeed and t_{db} have greater impact on the measured temperature (Bond & Kelly, 1955; Kuehn, Stubbs, & Weaver, 1970). ISO 7726 standard (ISO 7726, 2001) describes calculation of t_{mr} in moderate TEs for several sphere diameters. Valid ranges of airspeed and t_{db} ranges are not specified and inclusion of combined uncertainty in globe temperature (t_g) measurement is neglected.

Standard BGTs have been implemented in indoor and outdoor human thermal comfort assessments (Fanger & others, 1970; Gagge, Fobelets, & Berglund, 1986; Thorsson, Lindberg, Eliasson, & Holmer, 2007) and for livestock heat stress studies (Blackshaw & Blackshaw, 1994; Bond, Kelly, Garrett, & Hahn, 1961; Nienaber, Hahn, & Eigenberg, 1999; Purswell & Davis, 2008). Smaller globes were theoretically analyzed (Hey, 1968), but lacked experiment evaluation. Graves (1974) simulated numerous TEs and found smaller diameter BGTs to be valid for a range of TE conditions. Other approaches included using ping-pong balls as spheres (De Dear, 1987; Pereira, Bond, & Morrison, 1967), while Hetem, Maloney, Fuller, Meyer, & Mitchell (2007) developed and corrected a miniglobe temperature to the standard diameter t_g in a custom calibration chamber capable of simulating different TEs for use on ungulates. Custom experimental systems have also been developed to study asymmetric radiant temperatures (Fontana, 2010).

The standard BGT is too large and expensive (especially if multiple are needed) to evaluate TE spatial and temporal distributions in swine barns. Further, with the lack of confident data for the effects of convection for smaller diameter spheres, the valid ranges of these equations, and BGT calibration procedures, a novel calibration system named Animal Thermal Environment Replication and Measurement System (AThERMS) was developed and commissioned to calibrate BGTs. To achieve these goals, the objectives were:

1. Design and construct a novel system capable of generating and controlling a range of TE conditions,
2. Perform functional performance testing on surface temperatures and airspeed, and
3. Determine time constant to heat and cool the surfaces.

Materials and Methods

Chamber Design and Construction

Animal Thermal Environment Replication and Measurement System (AThERMS; figure 1; figure 2; figure 3) was designed to calibrate BGTs (or any other TE sensor) by simulating different radiative, convective, and evaporative TEs a housed animal may experience. Different t_{db} , RH, and airspeeds were allowed to be simulated at the center of a large chamber constructed of 0.7 mm (0.0276 in.) thick sheet metal painted gloss white (assumed emissivity of 0.92) to replicate a “grey” body. Interior dimensions (L x W x H; figure 3) were 1.04 x 1.17 x 1.04 m (41 x 46 x 41 in.). All six sides of the chamber (>90% area in thermal radiation exchange with the BGT) were maintained at the same surface temperature (t_s). The inlet featured a 0.15 m (6 in.) diameter opening with a 4.77 mm (0.188 in.) perforated hole diameter diffuser, to straighten the flow and increase the surface area of the wall (as opposed to leaving the inlet open). The outlet consisted of a 0.20 m (8 in.) diameter opening, with 6.35 mm (0.25 in.) hole perforated hole diameter diffuser mounted in the center of the wall opposite the inlet (figure 1). The inlet and outlet were sealed with weather stripping and the interior of the chamber was sealed with silicone. An access door (figure 2), sealed with weather stripping, was cut on the inlet side to allow entrance. AThERMS was placed in a large Insulated Enclosure (IE; figure 1) constructed of 0.051 m (2 in.) thick rigid foam board insulation (R-10) with exterior dimensions (L x W x H) of 2.44 x 2.44 x 1.83 m (8 x 8 x 6 ft). Concentric ring diffusers placed on opposite sides of the IE distributed air around AThERMS, inside the IE to control t_s (figure 1). A 0.15 m (6 in.) diameter outlet (top of the IE) returned air back (figure 1) to the Air Handling Unit (AHU; figure 1) with make-up air from the room available when required. A t_{db} and RH sensor (HMP-133Y, Vaisala, Helsinki, Finland) was located near the return in the IE.

The AHU (figure 1; AA-5474, Parameter Generation and Control, Black Mountain, NC, USA) conditioned air (at a set t_{db} and RH) supplied to both AThERMS (figure 2) and IE (figure 1) through a 0.15 m (6 in.) diameter duct split via a wye with flow controlled to AThERMS by an actuated damper (figure 1; figure 2; remaining flow went to the IE diffusers). Maximum flow provided by the AHU was $0.33 \text{ m}^3 \text{ s}^{-1}$ (700 cfm) with 3000 W (10236 BTU h^{-1}) sensible heating and 5275 W (1.5 ton) cooling capacity.

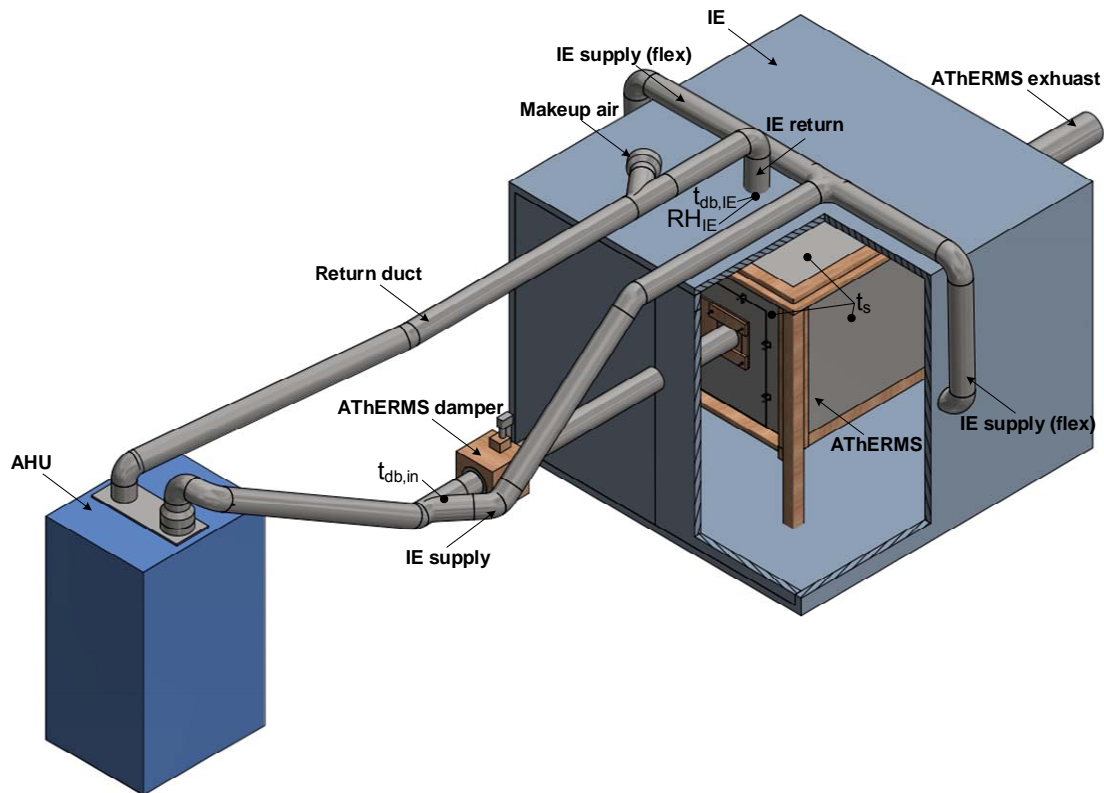


Figure 1. Schematic of AHU, IE, and AThERMS. Conditioned air from AHU to AThERMS was controlled by an actuated damper with excess flow supplied to each side of IE via flex duct (modeled as rigid for simplicity). AThERMS exhausted air to the room and air circulating around AThERMS and inside IE was returned back to AHU.

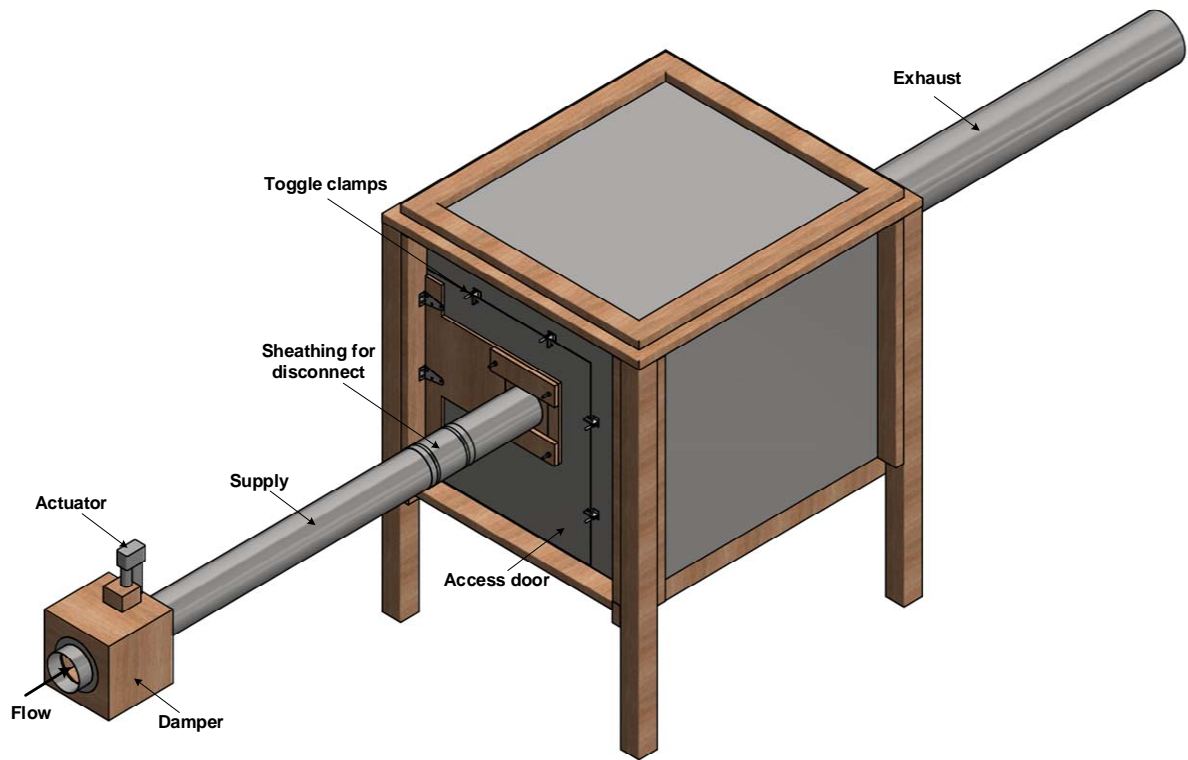


Figure 2. Detailed schematic of AThERMS from figure 2. An actuated damper controlled flow from AHU, supplied via rigid duct. A sheathing secured by hose clamps connected the access door duct to the supply duct. Toggle clamps secured the weather-stripped access door in place.

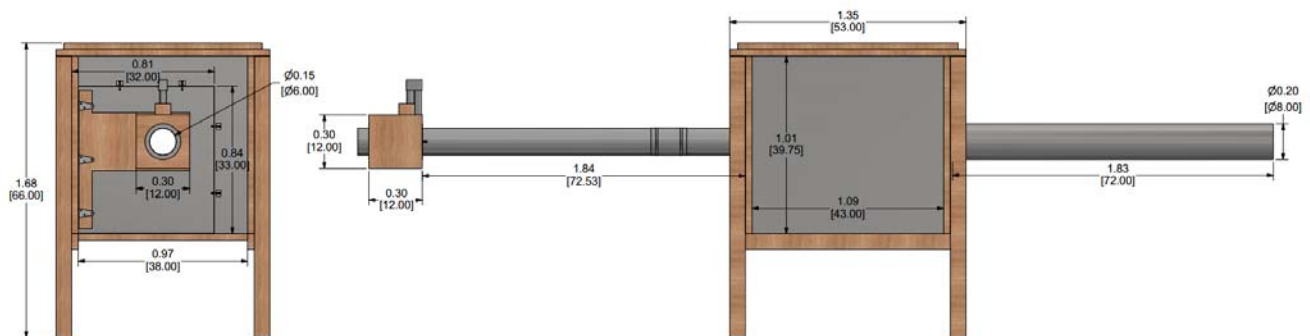


Figure 3. Dimensioned drawing of AThERMS (figure 2). All units in meters [in.].

Thermal Environment Performance Testing

Upon completion of AThERMS and IE construction, but prior to initiating BGT calibration, AThERMS performance was verified to provide a consistent and stable TE.

Airspeed

Flow through AThERMS was visualized using smoke (S102, Regin HVAC Products, Inc., Oxford, CT, USA) injected into the supply duct and recorded with a small video camera. Light sources were placed on the bottom of the chamber and black background was added opposite of the camera to aid in visualization of the flow patterns.

Three nominal supply flowrates: (i) low, (ii) medium, and (iii) high, controlled by the actuated damper (figure 1; figure 2), were used to evaluate airspeeds (commonly found in swine facilities) and Turbulent Intensity (TI) in the central region (figure 4a) of AThERMS. A three-dimensional traverse (figure 4) was conducted using a hot-wire anemometer (Model 8455, TSI Inc., Shoreview, MN, USA) across an 0.25 x 0.25 x 0.20 m (10 x 10 x 8 in.)

volume. Three 12 V_{DC} linear actuators (HDA10-2 and HDA8-2, Robotzone LLC., Winfield, KS, USA) moved the anemometer in the x, y, and z directions (figure 4b), and ~243 measurement locations were randomly tested. Velocity was assumed only in the y-direction (figure 4a) based on smoke visualization. Position of anemometer relative to center of the chamber was determined by calibrating actuator displacement against the analog response (from an internal 10kΩ potentiometer) and measuring the offset for the side and bottom surfaces. Six airspeeds per measurement location were sampled every second from the anemometer, which internally calculates the average every 50 ms. Average velocity at each measurement location was used to determine TI and construct a three-dimensional velocity profile using three-dimensional linear interpolation of a 5 mm (0.2 in.) mesh grid (*Matlab*, 2015). All tests were conducted at a constant $t_{db,in}$ (20°C) and RH_{in} (50%).

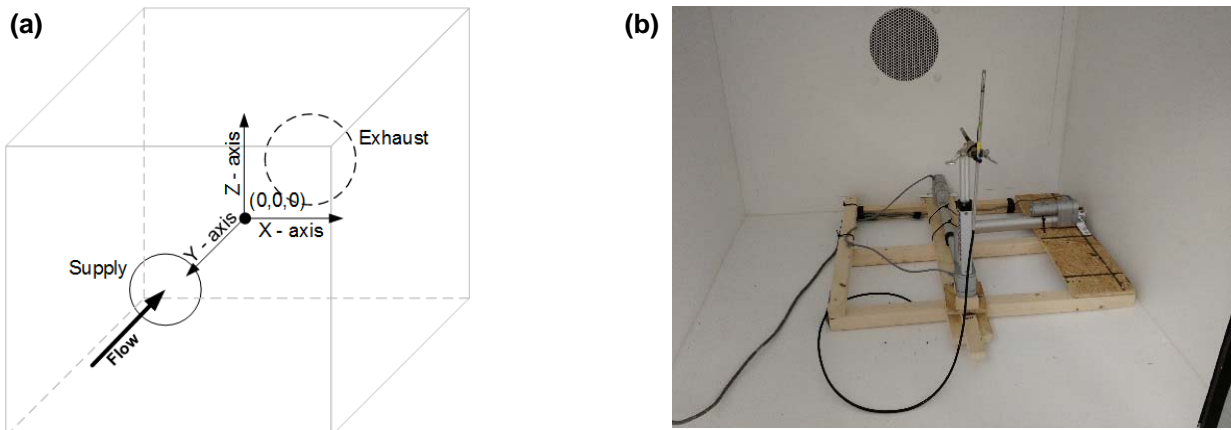


Figure 4. (a) Coordinate system for airspeeds measurements with the origin at the center of the chamber. (b) Three linear actuators used to complete three-dimensional airspeed traverse in the center (location of BGT) using a hot-wire anemometer.

A Computational Fluid Dynamics (CFD) model was developed to compare with two aforementioned flow visualization methods. AThERMS was initially modeled (*Inventor*, 2015) to scale and imported into *Fluent* (2015). To decrease computation time and complexity, the outlet perforated plate was simplified by using larger holes. A $k-\epsilon$ RNG with standard wall functions viscous model was used with absolute velocity formation and a pressure-based solver. Boundary Conditions (BCs) were specified at 0.762 m (3 in.) upstream of the inlet and 0.762 m (3 in.) downstream of the outlet of AThERMS. Inlet BCs consisted of velocity, pressure, and turbulence, which were measured during traverse testing. Outlet BCs contained pressure and turbulence, also verified during traverse testing. Pressure-velocity coupling was solved using the SIMPLE algorithm.

Surface and Dry-Bulb Temperature

A stable and evenly distributed t_s on each of the six sides of AThERMS was verified using six digital infrared (IR) temperature sensors (MLX90614, Melexis NV, Leper, Belgium) each mounted to a surface of a small cube (figure 5a) suspended in the center of AThERMS (figure 5b) and set to record t_s every 6 s (Uno R3, Arduino Inc., Italy). IR cube placement was verified to not impact t_s prior to testing by placing the IR cube in the center of AThERMS. The IR sensors were calibrated by the manufacturer with an emissivity of 1.0, which was assumed to match the emissivity of the painted surfaces in AThERMS. Mean IR t_s was analyzed during the steady-state phase for nominal AHU supply set points ($t_{db,in}$): (i) 13°C (55.4°F), (ii) 23°C (73.4°F), (iii), 33°C (91.4°F). An uncertainty analysis (table 1) was performed for the IR sensor to establish the confidence in t_s . Standard uncertainties obtained from the Type B evaluation were much greater than the Type A evaluation (i.e., standard error); thus, standard error was neglected but still identified to emphasize its importance (table 1).

Ambient temperature stability was confirmed by using a t_{db} sensor (NTCLE413E2 thermistor, Vishay Intertechnology Inc., Malvern, PA, USA) located near the center of AThERMS. A datalogger (Micro, Arduino LLC, Italy) sampled t_{db} every 2 s and was recorded with custom developed software (Python 2.7).

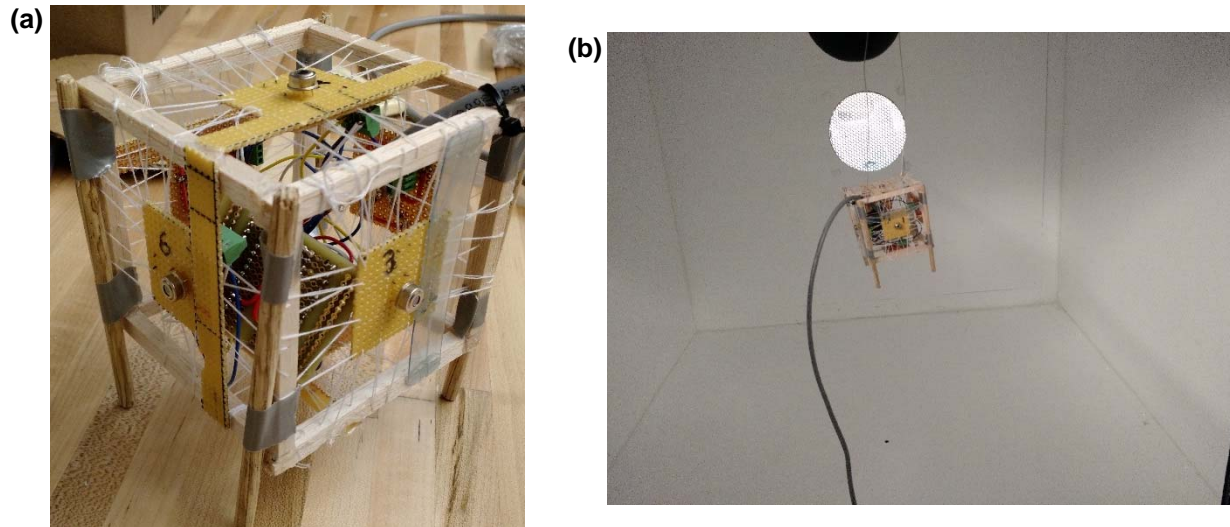


Figure 5. (a) Close up of six digital IR sensors mounted on each surface of a cube and (b) suspended in the center of ATHERMS.

Table 1. Uncertainty analysis for digital IR sensor. Standard error was very small relative to other standard uncertainties; thus, neglected.

Source	Value (°C)	Probability distribution	Divisor	Standard uncertainty (°C)
Standard Error	-	Normal	1	-
Reading Resolution ^[1]	0.01	Rectangular	$\sqrt{3}$	8.33E-6
Accuracy ^[2]	0.5	Rectangular	$\sqrt{3}$	0.083
Measurement Resolution ^[3]	0.02	Rectangular	$\sqrt{3}$	0.003
Combined standard uncertainty				0.29
Coverage factor, $k^{[4]}$				2
Expanded uncertainty				0.58

^[1] indicated t_s can lie with equal probability anywhere in the interval $t_s - 0.005$ to $t_s + 0.005$

^[2] range: 0°C to 50°C

^[3] SMBus protocol resolution, indicated t_s can lie with equal probability anywhere in the interval $t_s - 0.01$ to $t_s + 0.01$

^[4] approximately 95% confidence interval and infinite degrees of freedom

A nonlinear least squares regression (*Matlab*, 2015) of mean t_s (i.e., all six sides averaged) versus elapsed time was performed to determine the time constant (τ , ~63%) for heating and cooling the system. The time constants served as a metric to determine the time to reach steady-state. The time to reach steady-state was estimated by 3τ (~95% of the steady-state value), assuming first-order system behavior (equation 1).

$$t_s(t) = t_{s,0} + \Delta t_s \left(1 - e^{-\frac{t-t_0}{\tau}} \right) \quad (1)$$

where

- $t_s(t)$ = surface temperature as a function of time (°C)
- $t_{s,0}$ = initial t_s at time t_0 (°C)
- Δt_s = difference between $t_{s,0}$ and t_s at steady-state (°C)
- t = time (min)
- t_0 = initial time (min)
- τ = time constant (min^{-1})

Results and Discussion

Chamber Performance Testing

Airspeed

Flow visualization with smoke and the CFD model confirmed the magnitude of velocity to be predominately in the y-direction (figure 6). Although some smoke swirls in the center of AThERMS, a steady jet forms in the y-direction. In addition, flow pattern formation and distribution shown by the smoke was similar to the CFD model (figure 6d). As air entered AThERMS, it forms a jet that carries through to the outlet (figure 6a). Some air collides with the outlet wall and recirculates back contribute to forming the jet (figure 6b).

Each of the three nominal supply flowrates tested (low, medium, high), showed consistent velocity profiles in the central region of AThERMS (figure 7). Simulations showed flow patterns similar to the CFD model; however, the magnitude of the velocity differed slightly. More work is needed to further develop the CFD model and to ensure the BCs are representative of the experimental BCs.

These results aided in determining possible locations of the omnidirectional airspeed sensor (accompanies BGT) that accurately reflects the typical convective environment experienced by the BGT. The omnidirectional airspeed sensor must not impact t_{mr} measurement or measure airspeed in the boundary region around the sphere. The optimum location is the best estimate of the “free stream” airspeed passing the ball. Albeit, control of and uniform flow patterns are not possible in the end application of this instrument (i.e., swine facilities). The sources of forced convection in swine barns (e.g., fans or open curtains) do create large regions of similar airspeeds such that precise measurement is not required but is desired during BGT calibration. Based on the observed velocity patterns from both the traverse and CFD model, the omnidirectional airspeed sensor should be placed near the side of the BGT.

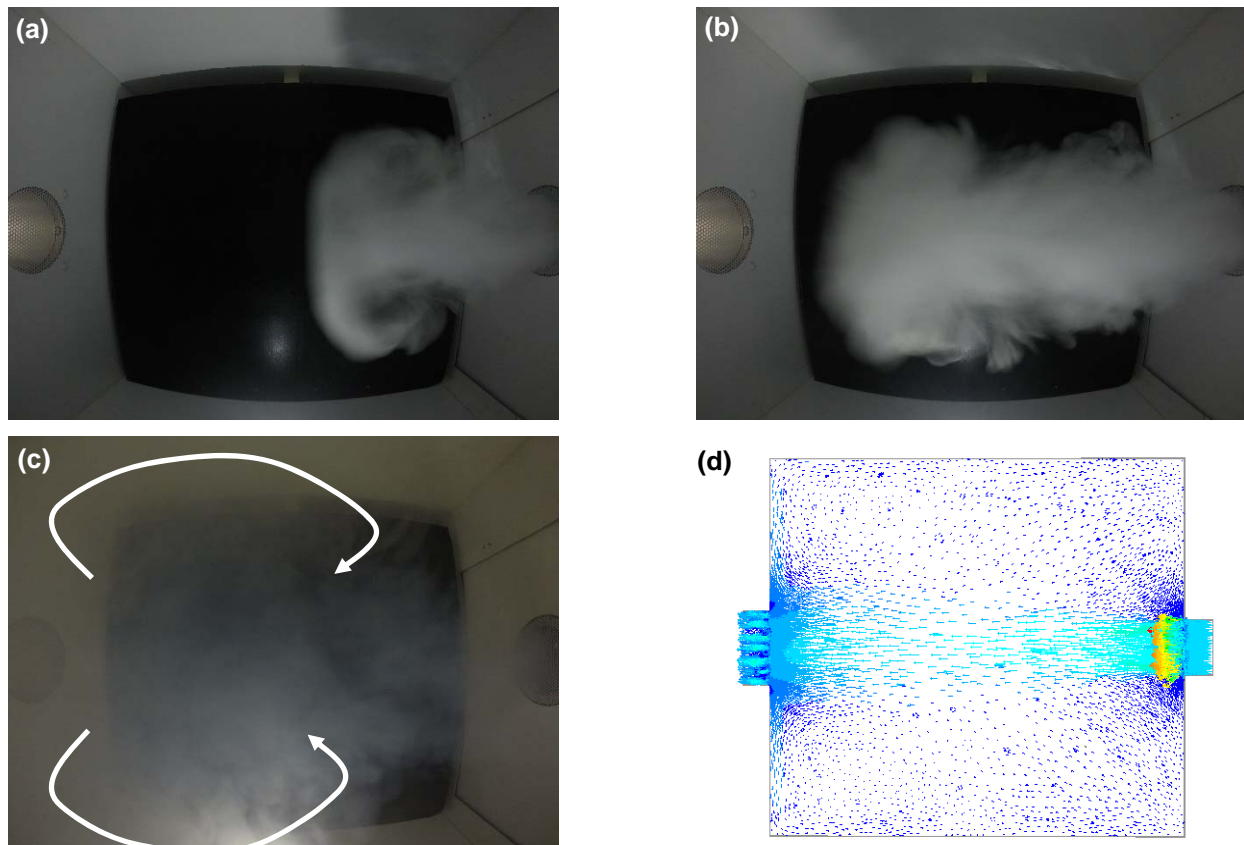


Figure 6. At a nominal low flow, (a) smoke initially entering AThERMS and (b) formation of the jet. (c) Some smoke circulates back to the jet as confirmed in the (d) CFD model showing theoretical flow vectors (colored by velocity magnitude).

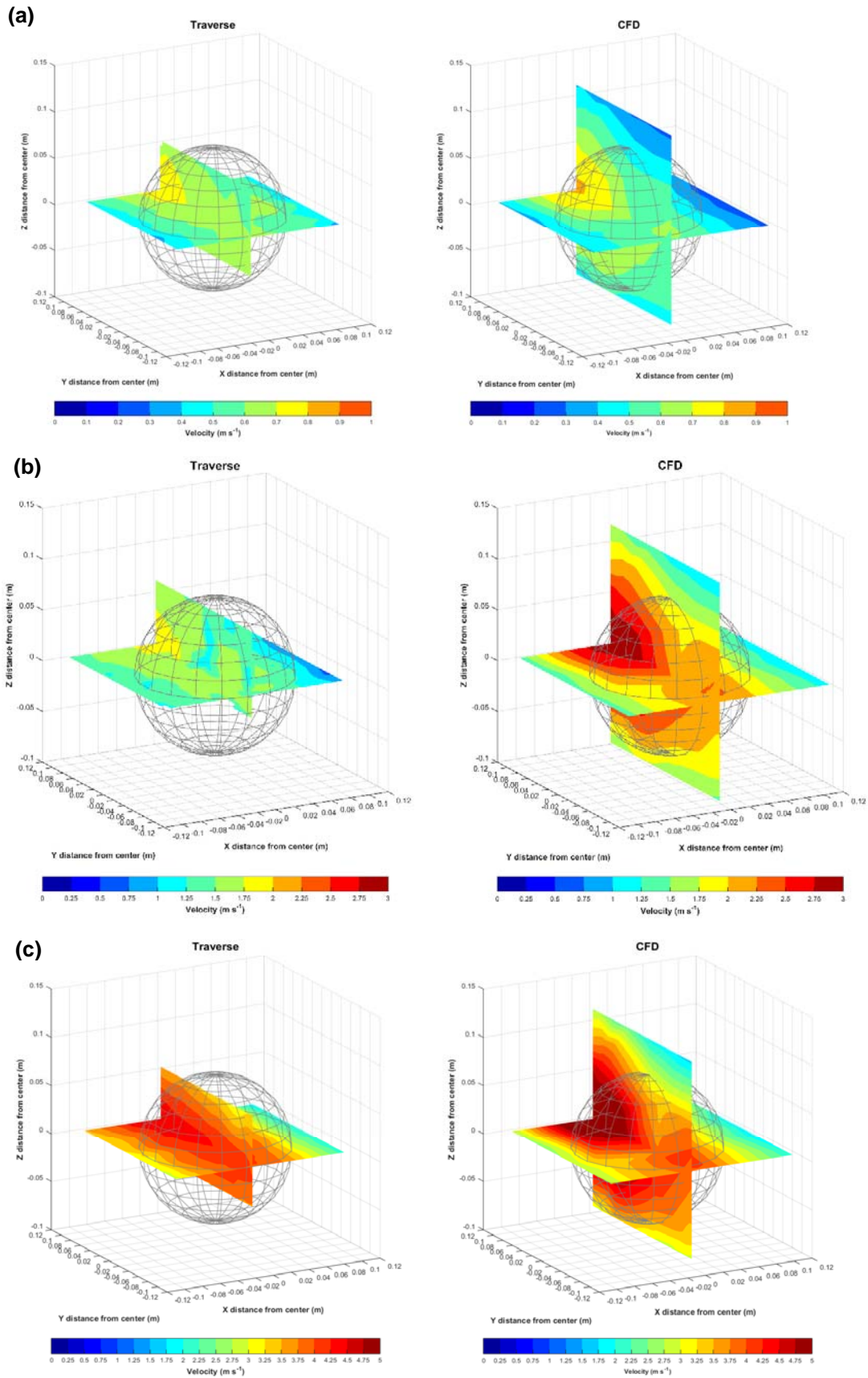


Figure 7. Velocity visualization for low (a), medium (b), and high (c) nominal supply flowrates. CFD simulations varied from the traverse and simulated higher velocities at the BGT.

Surface and Dry-Bulb Temperature

All six interior surfaces of AThERMS were found to provide uniform and stable surface temperatures (t_s) at the three nominal supply air temperatures ($t_{db,in}$) tested (figure 8; table 2). At 23°C $t_{db,in}$ (figure 8b), mean t_s was very similar to mean $t_{db,in}$ (supplied to both AThERMS and IE), while for the 13°C (figure 8a) and 33°C (figure 8c) $t_{db,in}$, mean t_s was higher and lower than the $t_{db,in}$, respectively. This difference was most likely attributed to heat loss through the uninsulated supply ducts and the IE. Ambient dry-bulb temperature of the room housing the IE and AThERMS was approximately 22°C and flow to AThERMS was about 0.0064 m³ s⁻¹ (13.5 CFM) while the remaining flow went to the IE (increases heat losses through the supply ducts). This explanation also rationalizes the difference between $t_{db,in}$ and $t_{db,IE}$. At 23°C, mean t_s was very similar to mean temperature inside AThERMS ($t_{db,bgt}$), while at 13°C and 33°C, mean t_s was lower and higher than the $t_{db,bgt}$, respectively. Albeit, this difference is not statistically significant based on the standard uncertainties of the two measurement sensors and data acquisition systems. A possible explanation may be due to a slight difference in assumed emissivity of the digital IR sensor and the actual emissivity of the white surface or the influence of temperature on the digital IR sensor measurement. Further, these results simplify the thermal radiation network from seven nodes (six surfaces plus the BGT) to a trivial two-node problem, since all six t_s are equal there is not thermal radiation exchange. This corroborates the theoretical assumption of the “large enclosure” scenario, where the surroundings are a uniform temperature.

A stable temperature inside AThERMS ($t_{db,bgt}$) was observed for each of the three nominal AHU set points (table 2) indicating consistent input of t_{db} into determining convective heat transfer coefficients for the BGT. Low fluctuations in $t_{db,in}$ from the AHU considerably aided in maintaining stable t_s and $t_{db,bgt}$.

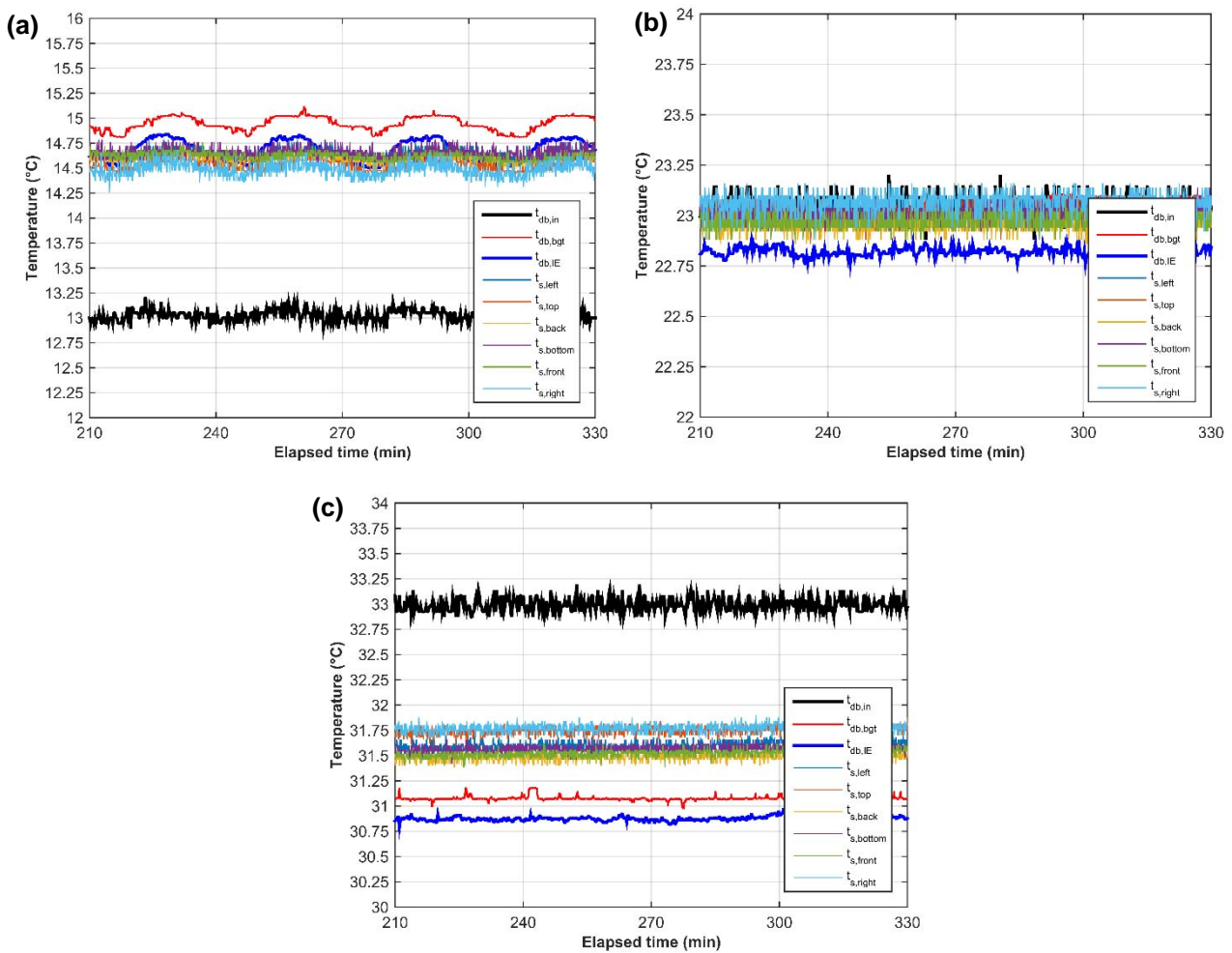


Figure 8. For three nominal AHU supply set point temperatures ($t_{db,in}$), (a) 13°C, (b) 23°C, and (c) 33°C, results showed uniform and stable surface temperature and AThERMS dry-bulb temperature.

Table 2. Mean (\pm standard deviation) of steady-state temperatures at three nominal supply set point temperatures.

Surface ID ^[1]	Nominal AHU supply temperature ($^{\circ}$ C)		
	13	23	33
$t_{s, \text{left}}$	14.66 \pm 0.05	23.03 \pm 0.03	31.66 \pm 0.11
$t_{s, \text{top}}$	14.54 \pm 0.05	23.01 \pm 0.04	31.81 \pm 0.10
$t_{s, \text{back}}$	14.60 \pm 0.05	22.96 \pm 0.04	31.55 \pm 0.11
$t_{s, \text{bottom}}$	14.65 \pm 0.05	23.01 \pm 0.04	31.63 \pm 0.10
$t_{s, \text{front}}$	14.61 \pm 0.05	22.97 \pm 0.04	31.58 \pm 0.11
$t_{s, \text{right}}$	14.49 \pm 0.07	23.07 \pm 0.05	31.83 \pm 0.10
$t_{\text{db, in}}$ ^[2]	13.03 \pm 0.06	23.03 \pm 0.06	33.00 \pm 0.07
$t_{\text{db, IE}}$ ^[3]	14.67 \pm 0.11	22.82 \pm 0.02	30.97 \pm 0.13
$t_{\text{db, bgt}}$ ^[4]	14.95 \pm 0.07	23.06 \pm 0.03	31.17 \pm 0.13

^[1] n = 2898

^[2] n = 480

^[3] n = 481

^[4] n = 7610

Time to reach steady-state (3τ) was 85.2 min (cooling) and 42.0 min (heating; table 3). Coefficients of determination (R^2) were greater than 0.97 for each regression (figure 9). The Root Mean Square Error (RMSE) provided an estimate of the overall uncertainty over the regression. Heating caused the system to reach steady-state faster compared with cooling, due to the equipment in the AHU. Sensible heat was directly transferred to the air by five looped coils, whereas for cooling, air passes through an evaporative cooling spray chamber. Time to reach steady-state was used to improve experimental and operational protocols when the BGT or any other sensor were inside the AThERMS.

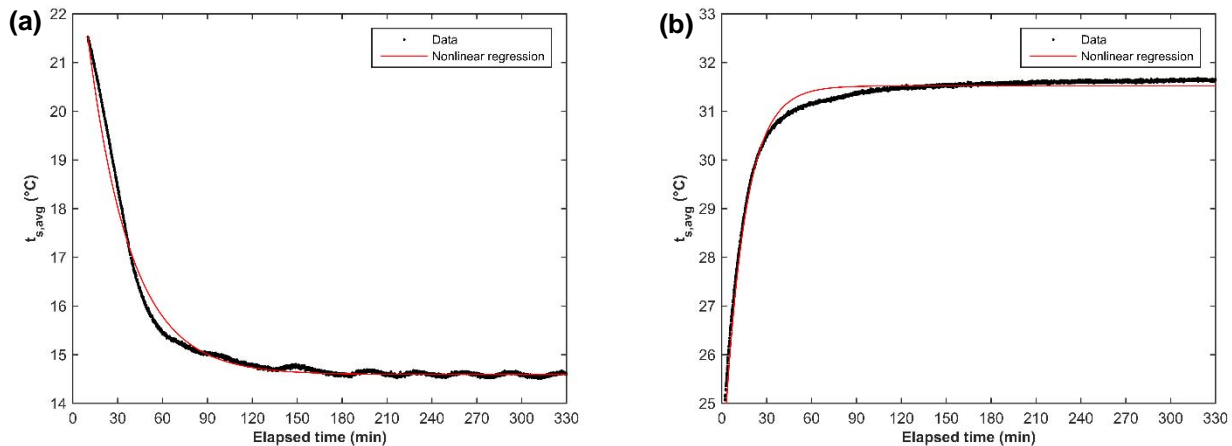


Figure 9. Nonlinear regression to determine the time constant for cooling (a) and heating (b) AThERMS.

Table 3. Nonlinear regression coefficients and statistics summary to estimate the time to reach steady state (3τ) for cooling and heating AThERMS.

Nominal AHU supply temperature ($^{\circ}$ C)	$t_{s,0}$ ($^{\circ}$ C)	Δt ($^{\circ}$ C)	t_0 (min)	R^2	RMSE ($^{\circ}$ C)	Time to reach steady-state (min)
13	21.5	-6.98	10.05	0.986	0.1602	85.2
33	24.5	7.02	2.08	0.979	0.1364	42.0

The overall goal of AThERMS is to calibrate and validate a single device that contains several TE sensors that will be used to assess the functional performance of all the components impacting the spatial and temporal TE distribution in a swine facility (e.g., ventilation, supplemental heating, building envelope, inlets, etc.). This information will be used to identify uneven or poor TEs in Animal Occupied Zone (AOZs), in which suggestions for improving the TE can be generated.

Conclusions

A novel and well-documented TE simulation system named Animal Thermal Environment Replication and Measurement System (AThERMS) was developed. Simulations of different combinations of dry-bulb temperature, relative humidity, and airspeeds while independently controlling chamber surface temperature (t_s) were evaluated. AThERMS is a chamber inside a large Insulated Enclosure (IE) where air supplied by an air handling unit provides unique TEs to both AThERMS and the IE. Commissioning of AThERMS prior to BGT assessment included a qualitative (smoke visualization) and quantitative (three-dimensional traverse and CFD model) velocity characterization in the central region of the chamber and verification of similar and stable t_s for all six surfaces. Analysis of velocity contours sliced in different x, y, z planes surrounding the BGT at three nominal flowrates indicated steady patterns and helped guide placement of the airspeed sensor used to derive the impact of convection on measured BGT temperature.

AThERMS can be successfully used to simulate different TEs experienced in the AOZ inside livestock production system and function as a reference to calibrate or verify TE measurements. Further work is required to assess to isothermal and nonisothermal conditions (i.e., t_s differs from $t_{db,bgt}$) with a BGT present and evaluate the effects of convection on different diameter BGTs. Globe temperatures obtained from AThERMS will be compared to ISO 7726 standard and theoretical heat transfer models. AThERMS is the initial step in developing a network of TE measurement devices to monitor seasonal spatial and temporal distribution of TE inside swine facilities.

Acknowledgements

This research was supported with funding provided by the Iowa Pork Producers Association. The authors would like to acknowledge the contributions of undergraduate student Grant Hoppes during the preparation and completion of this work.

The research work of Yun Gao was partly supported by the Fundamental Research Funds for the Central Universities of China (2013PY052).

References

- Alfano, F. R., Dell'Isola, M., Palella, B. I., Riccio, G., & Russi, A. (2013). On the measurement of the mean radiant temperature and its influence on the indoor thermal environment assessment. *Building and Environment*, 63, 79–88. <http://doi.org/10.1016/j.buildenv.2013.01.026>
- ASHRAE. (2013). *Handbook of Fundamentals*. Atlanta, GA: America Society of Heating, Refrigeration and Air Conditioning Engineers.
- Beckett, F. E. (1965). Effective Temperature for Evaluating or Designing Hog Environments. *Transactions of the ASAE*, 8(2), 0163–0166. <http://doi.org/10.13031/2013.40457>
- Bedford, T., & Warner, C. G. (1934). The Globe Thermometer in Studies of Heating and Ventilation. *Epidemiology & Infection*, 34(04), 458–473. <http://doi.org/10.1017/S0022172400043242>
- Bjerg, B., Svidt, K., Zhang, G., & Morsing, S. (2000). SE—Structures and Environment: The Effects of Pen Partitions and Thermal Pig Simulators on Airflow in a Livestock Test Room. *Journal of Agricultural Engineering Research*, 77(3), 317–326.
- Blackshaw, J. K., & Blackshaw, A. W. (1994). Heat stress in cattle and the effect of shade on production and behaviour: a review. *Animal Production Science*, 34(2), 285–295.
- Bond, T. E., & Kelly, C. F. (1955). The globe thermometer in agricultural research. *Agricultural Engineering*, 36(4), 251–255.
- Bond, T. E., Kelly, C. F., Garrett, W. N., & Hahn, G. L. (1961). Livestock shades. *Calif. Agric*, 15(7), 7. Retrieved from <https://ucanr.edu/repositoryfiles/ca1507p7-64888.pdf>
- Bond, T. E., Kelly, C. F., & Heitman Jr, H. (1952). Heat and moisture loss from swine. *Agric. Eng*, 33(3), 1948–154.
- Boon, C. R., & Wray, C. (1989). Building design in relation to the control of diseases of intensively housed livestock. *Journal of Agricultural Engineering Research*, 43, 149–161.
- Curtis, S. E. (1983). *Environmental Management in Animal Agriculture*. Ames, IA: The Iowa State University Press.
- De Dear, R. (1987). Ping-pong globe thermometers for mean radiant temperatures. *Heating and Ventilating Engineer*, 60(681).
- DeShazer, J. A. (2009). *Livestock Energetics and Thermal Environmental Management* (1st ed.). St. Joseph, MI: American Society of Agricultural and Biological Engineers.
- DeShazer, J. A., & Yen, J.-T. (2009). Chapter 3: Energetics of Biological Processes. In James A. DeShazer, *Livestock Energetics and Thermal Environment Management* (1st ed., pp. 49–71). St. Joseph, MI: American Society of Agricultural and Biological Engineers.
- Fanger, P. O., & others. (1970). Thermal comfort. Analysis and applications in environmental engineering. *Thermal Comfort. Analysis and Applications in Environmental Engineering*.
- Fluent. (2015). (Version 16.0). Ansys Inc.
- Fontana, L. (2010). Experimental study on the globe thermometer behaviour in conditions of asymmetry of the radiant

- temperature. *Applied Thermal Engineering*, 30(6–7), 732–740. <http://doi.org/10.1016/j.applthermaleng.2009.12.003>
- Gagge, A. P., Fobelets, A. P., & Berglund, L. G. (1986). A Standard Predictive Index of Human Response to the Thermal Environment. *ASHRAE Trans.*; (United States), 92:2B.
- Gentry, J. G., McGlone, J. J., Miller, M. F., & Blanton, J. R. (2004). Environmental effects on pig performance, meat quality, and muscle characteristics. *Journal of Animal Science*, 82(1), 209–217.
- Graves, K. W. (1974). Globe Thermometer Evaluation. *American Industrial Hygiene Association Journal*, 35(1), 30–40. <http://doi.org/10.1080/0002889748507003>
- Hellon, R. F., & Crockford, G. W. (1959). Improvements to the globe thermometer. *Journal of Applied Physiology*, 14(4).
- Hetem, R. S., Maloney, S. K., Fuller, A., Meyer, L. C. R., & Mitchell, D. (2007). Validation of a biotelemetric technique, using ambulatory miniature black globe thermometers, to quantify thermoregulatory behaviour in ungulates. *Journal of Experimental Zoology Part A: Ecological Genetics and Physiology*, 307A(6), 342–356. <http://doi.org/10.1002/jez.389>
- Hey, E. N. (1968). Small globe thermometers. *Journal of Physics E: Scientific Instruments*, 1(9), 955. <http://doi.org/10.1088/0022-3735/1/9/424>
- Hillman, P. E. (2009). Chapter 2: Thermoregulatory Physiology. In *Livestock Energetics and Thermal Environment Management* (1st ed., pp. 23–48). St. Joseph, MI: American Society of Agricultural and Biological Engineers.
- Inventor. (2015). Autodesk Inc.
- ISO 7726. (2001). *Ergonomics of the thermal environment — instruments for measuring physical quantities*. Geneva: International Standardization Organization.
- Jerez, S. B., Wang, X., & Zhang, Y. (2014). Quantification of Ventilation Effectiveness for Air Quality Control in Animal Buildings. *ASHRAE Transactions*, 120(1), 460–468.
- Kuehn, L. A., Stubbs, R. A., & Weaver, R. S. (1970). Theory of the globe thermometer. *Journal of Applied Physiology*, 29(5), 750–757.
- Lammers, P. J., Kenealy, M. D., Kliebenstein, J. B., Harmon, J. D., Helmers, M. J., & Honeyman, M. S. (2012). Energy use in pig production: an examination of current Iowa systems. *Journal of Animal Science*, 90(3), 1056–1068. <http://doi.org/10.2527/jas.2010-3782>
- Matlab. (2015). (Version R2015a). MathWorks.
- Mount, L. E. (1964). Radiant and convective heat loss from the new-born pig. *The Journal of Physiology*, 173(1), 96–113.
- Mount, L. E. (1967). The heat loss from new-born pigs to the floor. *Research in Veterinary Science*, 8(2), 175–186.
- Mount, L. E. (1975). The assessment of thermal environment in relation to pig production. *Livestock Production Science*, 2(4), 381–392. [http://doi.org/10.1016/0301-6226\(75\)90121-9](http://doi.org/10.1016/0301-6226(75)90121-9)
- Nienaber, J. A., Hahn, G. L., & Eigenberg, R. A. (1999). Quantifying livestock responses for heat stress management: a review. *International Journal of Biometeorology*, 42(4), 183–188. <http://doi.org/10.1007/s004840050103>
- Pereira, N., Bond, T. E., & Morrison, S. R. (1967). Ping-pong ball into black-globe thermometer. *Agricultural Engineering*, 48(6), 341.
- Purswell, J. L., & Davis, J. D. (2008). Construction of a low cost black globe thermometer. *Applied Engineering in Agriculture. ASABE*, 24(3), 379–381.
- Randall, J. M. (1993). Environmental parameters necessary to define comfort for pigs, cattle and sheep in livestock transporters. *Animal Science*, 57(02), 299–307. <http://doi.org/10.1017/S0003356100006929>
- Straw, B. E., Zimmerman, J. J., D'Allaire, S., & Taylor, D. J. (1999). *Disease of swine*. Iow state press, Ames, Iowa, USA.
- Thorsson, S., Lindberg, F., Eliasson, I., & Holmer, B. (2007). Different methods for estimating the mean radiant temperature in an outdoor urban setting. *International Journal of Climatology*, 27(14), 1983–1993.
- Vernon, H. M. (1932). The measurement of radiant heat in relation to human comfort. *Journal of Industrial Hygiene*, 14(3), 95–111.
- Wang, A., Zhang, Y., Sun, Y., & Wang, X. (2008). Experimental study of ventilation effectiveness and air velocity distribution in an aircraft cabin mockup. *Building and Environment*, 43(3), 337–343.
- Zhang, Y., Barber, E. M., & Ogilvie, J. R. (1988). Simulation of the dynamic thermal environment in a swine barn. *American Society of Agricultural Engineers*.

Nomenclature

AThERMS (Animal Thermal Environment Replication and Measurement System)

IE (Insulated Enclosure)

AHU (Air Handling Unit)

Dry-bulb temperature (t_{db})

Relative Humidity (RH)

Surface temperature (t_s)